NAVAL POSTGRADUATE SCHOOL
Monterey, California

THESIS

OCEAN WAVE HEIGHT TRANSFORMATION MODEL
USING
SURFACE ROLLER THEORY

by

A. Henry Brookins

June, 1993

Thesis Advisor: Edward B. Thornton

Unclassified

Security Classification of this page

REPORT DOCUMENTATION PAGE

1a Report Security Classification: Unclassified		1b Restrictive Markings	
2a Security Classification Authority		3 Distribution/Availability of Report	
2b Declassification/Downgrading Schedule		Approved for public release; distribution is unlimited.	
4 Performing Organization Report Number(s)		5 Monitoring Organization Report Number(s)	
6a Name of Performing Organization Naval Postgraduate School	6b Office Symbol *(if applicable)* 35	7a Name of Monitoring Organization Naval Postgraduate School	
6c Address *(city, state, and ZIP code)* Monterey CA 93943-5000		7b Address *(city, state, and ZIP code)* Monterey CA 93943-5000	
8a Name of Funding/Sponsoring Organization	6b Office Symbol *(if applicable)*	9 Procurement Instrument Identification Number	
Address *(city, state, and ZIP code)*		10 Source of Funding Numbers	
		Program Element No / Project No / Task No / Work Unit Accession No	

11 Title *(include security classification)* OCEAN WAVE HEIGHT TRANSFORMATION MODEL USING SURFACE ROLLER THEORY (UNCLASSIFIED)

12 Personal Author(s) A. Henry Brookins

13a Type of Report Master's Thesis	13b Time Covered From To	14 Date of Report *(year, month, day)* June 1993	15 Page Count 49

16 Supplementary Notation The views expressed in this thesis are those of the author and do not reflect the official policy or position of the Department of Defense or the U.S. Government.

17 Cosati Codes			18 Subject Terms *(continue on reverse if necessary and identify by block number)*
Field	Group	Subgroup	surface roller, bore dissipation, wave height , energy flux balance

19 Abstract *(continue on reverse if necessary and identify by block number)*

A wave height transformation model is developed using surface roller theory. Roller energy production is included in the energy flux balance equation to predict rms wave height for randomly varying, irregular waves over arbitrary bathymetry. The dissipation function is defined using wave roller theory, where the area of the roller is defined from a simple bore analogy. The Rayleigh distribution is used to statistically describe wave heights as waves shoal, break, and dissipate. Model predictions are compared with data acquired on both barred and near planar beaches. The surface roller wave height transformation model predicts rms wave heights with an average rms error of 6.5% for a barred beach over three days, 3.0% for two planar beaches over four days, and within 4.5% average error for all locations over seven days. The model has two free parameters, σ representing the type of breaker and γ a measure of breaking wave saturation, also a function of beach slope. Optimal values of both parameters are chosen by model fitting. The model is sensitive to γ, but not σ. The surface roller model improves the bore dissipation model [*Thornton and Guza*, 1983] by decreasing the average rms error by 40% while decreasing model sensitivity to input parameters.

20 Distribution/Availability of Abstract X unclassified/unlimited _ same as report _ DTIC users	21 Abstract Security Classification Unclassified	
22a Name of Responsible Individual Edward B. Thornton	22b Telephone *(include Area Code)* (408) 656-2847	22c Office Symbol 68TM

DD FORM 1473,84 MAR 83 APR edition may be used until exhausted

All other editions are obsolete

security classification of this page

Unclassified

Approved for public release; distribution is unlimited.

Ocean Wave Height Transformation Model
Using
Surface Roller Theory

by

A. Henry Brookins
Lieutenant, United States Navy
B.S., United States Naval Academy, 1986

Submitted in partial fulfillment
of the requirements for the degree of

MASTER OF SCIENCE IN METEOROLOGY AND PHYSICAL OCEANOGRAPHY

from the

NAVAL POSTGRADUATE SCHOOL
June 1993

Author: A. Henry Brookins

A. Henry Brookins

Approved by: Edward B. Thornton

Edward B. Thornton, Thesis Advisor

Thomas C. Lippmann

Thomas Lippmann, Second Reader

Curtis A. Collins

Curtis A. Collins, Chairman
Department of Oceanography

ABSTRACT

A wave height transformation model is developed using surface roller theory. Roller energy production is included in the energy flux balance equation to predict rms wave height for randomly varying, irregular waves over arbitrary bathymetry. The dissipation function is defined using wave roller theory, where the area of the roller is defined from a simple bore analogy. The Rayleigh distribution is used to statistically describe wave heights as waves shoal, break, and dissipate. Model predictions are compared with data acquired on both barred and near planar beaches. The surface roller wave height transformation model predicts rms wave heights with an average rms error of 6.5% for a barred beach over three days, 3.0% for two planar beaches over four days, and within 4.5% average error for all locations over seven days. The model has two free parameters, σ representing the type of breaker, and γ a measure of breaking wave saturation, also a function of beach slope. Optimal values of both parameters are chosen by model fitting. The model is sensitive to γ, but not σ. The surface roller model improves the bore dissipation model [*Thornton and Guza*, 1983] by decreasing the average rms error by 40% while decreasing model sensitivity to input parameters.

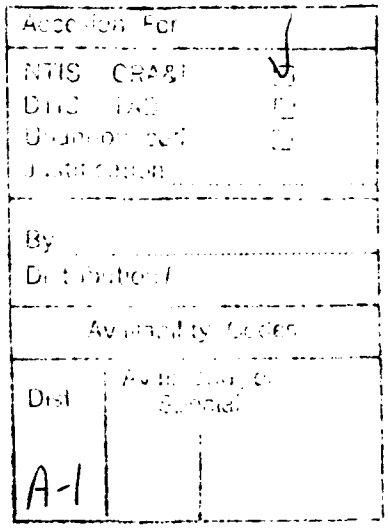

TABLE OF CONTENTS

I. INTRODUCTION

Wave heights gradually increase as waves shoal from deeper to shallower water. As waves propagate into very shallow water, they become unstable and break, generating turbulence at the surface boundary layer. The turbulence due to wave breaking is the primary dissipative mechanism causing wave energy decay in the surf zone. Dissipation rate and turbulent penetration depth are dictated by breaker type, commonly described as spilling, plunging, or surging. While plunging wave turbulence can penetrate to the bottom, spilling breaker turbulence is primarily confined to the surface layer between the crest and trough. Two important parameters which distinguish breaker type are wave steepness and beach slope.

Cacina, [1989] concluded that wave breaking is a function of both deep water wave steepness (H_0/L_0) and beach slope ($\tan\beta$), and is correlated with the deep water surf similarity parameter described by *Battjes* [1974] as

$$\zeta = \frac{\tan\beta}{\sqrt{\frac{H_{rms0}}{L_0}}} \tag{1}$$

where H_{rms0} is the deep water wave height, and L_0 is the deep water wave length ($gT^2/2\pi$).

Several methods have previously been employed to describe wave height distributions in the surf zone. The earliest models describe shoaling waves as monochromatic and entirely dependent on local water depth

$$H_{rms} = \gamma d \tag{2}$$

where γ is an adjustable coefficient, and d is local water depth. More recent wave height transformation models use the concept of energy flux balance and a physically based dissipation function. In the stochastic models of *Battjes and Janssen* [1978] and *Thornton and Guza* [1983] (TG83), wave heights are described statistically. Energy dissipation due to shallow water wave-breaking is modeled with simple periodic bores.

The objective of this paper is threefold: to improve the previously developed bore dissipation model by *Thornton and Guza*, [1983] by incorporating surface roller theory; to determine the influence of wave rollers on wave height transformation in the surf zone; and to reduce sensitivity to quasi-arbitrary model parameters. Waves are modeled as random, having irregular amplitude, and approaching from angles over arbitrary bottom profiles. Roller model generated wave heights are compared with observed wave heights acquired on a naturally barred beach during DELILAH (Duck, N.C., 1990), and on near-planar beaches from NSTS (Leadbetter Beach, Santa Barbara, 1978 and Torrey Pines Beach, San Diego, California, 1980).

II. SURFACE ROLLER MODEL

As the wave shoals, its height increases and the wave eventually breaks generating turbulent kinetic energy (tke) in a volume of water which becomes detached (separated) from the wave form and pitched forward down the wave face, defined as the wave roller. The surface roller is believed to play a vital role in wave height transformation within the surf zone [*Fredsoe and Deigaard,* 1992]. *Svendsen and Madsen* [1984] first modeled breaking waves as rollers, in which they envisioned a mass of water pushed by the wave front with horizontal velocity equal to the wave celerity C (Fig 1). The shear layer between the water in the roller and wave motion results in the dissipation of roller tke locally within the wave/roller system. Because the surface roller propagates with the wave, roller turbulence can be the main source of turbulence in the inner surf zone region [*Basco,* 1983].

The energy flux balance equation is used to determine wave energy gradients across the surf zone

$$\frac{\partial}{\partial x}(EC_g\cos\bar{\alpha}) = D \tag{3}$$

where E is energy, C_g is the wave group velocity, $\bar{\alpha}$ is the mean incident wave angle calculated using Snell's Law, and D is dissipation. As in TG83, the model assumes stationary wave conditions, straight and parallel bottom contours, and random waves which are narrow-banded in both frequency and direction (i.e., all waves are from the same direction and of a single frequency). Energy flux is contained in two terms, representing contributions from the wave, E_w, and the roller, E_r,

$$E = E_w + E_r \tag{4}$$

The dissipation term in Equation (1) is derived from the wave roller. Thus Equation (3) becomes

$$\frac{\partial}{\partial x}(E_w C_g \cos\bar{\alpha}) + \frac{\partial}{\partial x}(E_r C \cos\bar{\alpha}) = \epsilon_r \tag{5}$$

where ϵ_r represents roller dissipation.

Thornton and Guza [1983] show that wave height probability density functions both inside and outside the surf zone are well described by the Rayleigh distribution, p(H), where

$$p(H) = \frac{2H}{H_{rms}^2}\exp[-(\frac{H}{H_{rms}})^2] \tag{6}$$

The ensemble averaged wave energy, $<E_w>$, is calculated by integrating E_w through the Rayleigh distribution using linear wave theory

$$<E_w> = \frac{1}{8}\rho g \int_0^\infty H^2 p(H) d(H) = \frac{1}{8}\rho g H_{rms}^2 \tag{7}$$

where ρ is seawater density, g is gravitational acceleration, H is wave height, and H_{rms} is the root-mean-squared wave height. Group velocity, C_g, is described by linear wave theory

$$C_g = \frac{C}{2}(1 + \frac{2kd}{\sinh(2kd)}) \tag{8}$$

where C is phase velocity, d is depth, and k is the wavenumber associated with peak frequency $\bar{f}$ of the spectrum.

Surface roller energy is given by [*Svendsen*, 1984]

$$E_r = \frac{\rho A C^2}{2L} \tag{9}$$

where A is area of the roller and L is the wavelength of the wave. *Engelund* [1981] uses an analogy with a hydraulic jump to analytically determine roller area,

$$A = \frac{H^3}{4d\tan\sigma} \tag{10}$$

where σ is the angle of the roller/wave stress vector, τ, with respect to horizontal (Fig 1) . The value of σ is a function of breaker type and is believed to vary from a maximum value when breaking is initiated to a minimum value (estimated to be 10 degrees) in the inner surf zone [*Engelund*, 1981]. Thus Equation (9) becomes

$$E_r = \frac{\rho C \bar{f} H^3}{8d\tan\sigma} \tag{11}$$

The roller dissipation term, ε_r, represents work done on the roller per unit area per unit time, and is given by

$$\epsilon_r = \frac{\tau C}{L} = \rho g \bar{f} A \tan\sigma = \frac{\rho g \bar{f} H^3}{4d} \tag{12}$$

The work done by the roller is accomplished by the shear stress between the roller's bottom boundary and the wave's surface boundary, beginning at the toe (Fig 1). Turbulence generated at the toe moves horizontally through the top of the wave and fills the crest area as the roller slides down the wave face [*Bradshaw and Ferris*, 1965]. Turbulent kinetic energy is removed from the roller at the same rate.

Because the generation of turbulence and energy dissipation only apply to breaking waves, it is necessary to identify which waves are breaking. The average rate of energy dissipation, $<\epsilon_r>$, (as well as the average roller energy flux, E_r) is calculated by multiplying the dissipation for a single broken wave of height H by the probability of wave breaking at each height, $p_b(H)$, and integrating over all H [*Thornton and Guza*, 1983]. Breaking waves are identified by weighting the Rayleigh function for all waves, breaking and non-breaking

$$p_b(H) = W(H)p(H) \tag{13}$$

where $W(H)$ is a weighting function, and the area under the distribution $p_b(H)$ is equal to the percent of breaking waves. The weighting function is based empirically on acquired data which identify breaking waves, including both incipient breakers and rollers, and is given by

$$W(H) = \left(\frac{H_{rms}}{\gamma d}\right)^2 \left[1 - \exp\left(-\left(\frac{H}{\gamma d}\right)^2\right)\right] \tag{14}$$

$W(H) < 1$ unless conditions are totally saturated after which all waves break and $W(H)=1$.

Integrating H^3 in Equations (11) and (12) through the breaking wave height distribution yields

$$\langle H_b^3 \rangle = \int_0^\infty H^3 p_b(H) d(H) = \frac{3\sqrt{\pi}}{4} \frac{H_{rms}^5}{(\gamma d)^2} \left[1 - \frac{1}{(1 + (\frac{H_{rms}}{\gamma d})^2)}\right] \tag{15}$$

Using Equations (15), (11) and (7) in Equation (5) yields the ensemble averaged energy flux balance

$$\frac{\partial}{\partial x}(\frac{1}{8}\rho g C_g \cos\bar{\alpha} H_{rms}^2] + \frac{\partial}{\partial x}(\frac{3\sqrt{\pi}\rho C^2 \bar{f} \cos\bar{\alpha}}{32 d \tan\sigma} \frac{H_{rms}^5}{(\gamma d)^2}[1 - \frac{1}{1 + (\frac{H_{rms}}{\gamma d})^2}]) =$$

$$\frac{3\sqrt{\pi}\rho g \bar{f}}{16 d} \frac{H_{rms}^5}{(\gamma d)^2}[1 - \frac{1}{1 + (\frac{H_{rms}}{\gamma d})^2}]) \tag{16}$$

used to describe wave height transformation including a surface roller. For saturation conditions W(H)=1 (when all waves are breaking), the ensemble averaged breaker height reduces to

$$\langle H_b^3 \rangle = \frac{3\sqrt{\pi}}{4} H_{rms}^3 \tag{17}$$

simplifying the energy flux balance equation to

$$\frac{\partial}{\partial x}\left(\frac{1}{8}\rho g C_g \cos\bar{\alpha} H_{rms}^2\right) + \frac{\partial}{\partial x}\left(\frac{3\sqrt{\pi}\rho C^2 \bar{f}\cos\bar{\alpha}}{32d\tan\sigma} H_{rms}^3\right) = \frac{3\sqrt{\pi}\rho g \bar{f}}{16d} H_{rms}^3 \tag{18}$$

For saturation conditions, we must determine when the probability of all waves breaking is equal to one, or

$$\int_0^\infty p_b(H)d(H) = \int_0^\infty W(H)p(H)d(H) = 1 \tag{19}$$

Substituting Equations (6) and (14) into Equation (19) and solving for the shallow water depth limiting condition, saturation conditions exist when

$$\frac{H_{rms}}{\gamma d} = 1.27 \tag{20}$$

and Equation (18) is used instead of (16). A simple forward stepping numerical scheme is sufficiently accurate [*Thornton and Guza,* 1983] to solve Equations (16) and (18), written

$$(E_w C_{gx})_2 + (E_r C_x)_2 = \langle \epsilon_r \rangle_1 \Delta x + (E_w C_{gx})_1 + (E_r C_x)_1 \tag{21}$$

Due to the equation's nonlinear nature, $(H_{rms})_2$ (shoreward) must be solved iteratively given $(H_{rms})_1$, mean incident angle $\bar{\alpha}$, and mean frequency $\bar{f}$.

III. FIELD DATA

The surface roller model is verified by comparing data acquired during three field experiments conducted on two near-planar beaches of different slope (NSTS) and a barred beach (DELILAH). The experiments used extensive alongshore and cross-shore arrays of current meters and wave sensors. Only the cross-shore arrays are considered here. Days for data comparison are chosen from each experiment based on model assumptions of straight and parallel contours, steady state conditions, and narrow-bandedness in frequency and direction. Table 1 summarizes offshore wave and beach conditions for the days analyzed.

A. TORREY PINES BEACH, CALIFORNIA

The first NSTS experiment was held in November, 1978 at Torrey Pines Beach, located north of San Diego, California. Beach slope was approximately linear, varying between 1:50 in the surf zone to 1:20 in the swash region. Beach face topographies were generally concave-up and beach topography was relatively uniform in the alongshore direction.

A cross-shore array of 11 current meters, 4 pressure transducers, and 4 wave staffs were used to measure rms wave heights across the surf zone. Data were telemetered from the instruments at Torrey Pines to the Shore Processes Laboratory, Scripps Institution of Oceanography and digitally recorded at a rate of 64 samples per second. The data was then low-pass filtered and reduced to 2 samples per second [*Thornton and Guza,* 1983].

A wide variety of wave and weather conditions were encountered during the experiment. Significant offshore wave heights, H_0, varied between .6 and 1.6 meters. The average peak frequency of the incident wave spectra, $\overline{f_0}$, was fairly constant at 0.07 Hz ($\overline{T_p} \approx 14$s). Incident wave angles in 10-m depth were limited to less than 15 degrees due to offshore island shadowing and refraction [*Pawka et al.,* 1976]. Two days, 4 November and 10 November, are chosen for data comparison.

B. SANTA BARBARA, CALIFORNIA

The second NSTS experiment was conducted at Leadbetter Beach in Santa Barbara, California over a one month period in the winter of 1980. Bottom contours inside 6m depth were relatively straight and parallel. Mean nearshore beach slope varied between 1:33 and 1:16, depending on tide level.

A cross-shore array of 16 current meters and 6 pressure sensors measured the cross-shore wave transformation properties. Two wave slope arrays in deep water measured incident wave spectra. All instrument signals were cabled to shore and digitally recorded [*Thornton and Guza*, 1986].

Leadbetter Beach is oriented approximately east-west on a predominately north-south California coast. To reach Santa Barbara, the open-ocean North Pacific swell must pass between Point Conception and the Channel Islands, a narrow window of ±9 degrees centered on 249 degrees true [*Thornton and Guza*, 1986]. This unique beach orientation provided good data sets 3-6 February, of which days 4 and 5 are chosen for model comparison.

C. DELILAH

The third data set used was acquired on a barred beach during DELILAH held October 1-21, 1990 at the US Army Corps of Engineer's Field Research Facility at Duck, North Carolina. Both bar location and beach slope, which varied between 1:25 and 1:19, responded to a wide variety of wave conditions [*Church and Thornton*, 1993].

Directional wave spectra were obtained in 8m depth from an alongshore array of bottom mounted pressure sensors. A cross-shore array of 9 pressure sensors were located from 4m depth to the shoreline. The array provided near-continuous data throughout the experiment with a sampling rate of 8Hz. An autonomous Coastal Research Amphibious Buggy (CRAB) was used for daily bathymetric measurements.

Three days (Oct 10, 12, and 14) are cnosen for model comparison when waves were relatively narrow-banded, varying in rms wave height from .77 to 1.30 meters, and arriving at angles between 1 and 12 degrees from normal to the beach.

IV. MODEL RESULTS

Model results for representative days during each experiment are presented in Figures 2-8. The two free parameters, γ and σ, of the roller model are determined by fitting model H_{rms} to observed data in a least square sense. Optimal values for each day and the resultant percent rms error are given in Table 1. Root mean square error is determined at the wave height observation locations. The predicted and observed wave heights, and dissipation as a function of offshore distance and depth are shown in Figures 2a-8a. The gradient wave and gradient roller energy fluxes as a function of offshore distance and depth are shown in Figures 2b-8b. Dissipation (modeled by Equation (12)) in Figures 2a-8a is the sum of the gradient energy fluxes in Figures 2b-8b. The percent of breaking waves as a function of offshore distance and depth are shown in Figures 2c-8c.

The DELILAH results indicate two significant wave-breaking regions. The first region just seaward of the offshore bar is relatively broad, while the second region shoreward is more abrupt. Weather and wave conditions discussed earlier are evident. On October 10, relatively small waves with an average period of 9.1 seconds arrived at an average incident angle of 1.9 degrees. The tide level is .7m. As a result, only 55% of the waves break at the offshore bar. Some waves continue breaking as they propagate shoreward, until at approximately 20 meters offshore the remaining waves break and saturation occurs.

Waves began building on the 11th due to a remote storm and continue building through the 13th. By 12 October, larger waves are approaching with an average period of 15.6 seconds at incident angles up to 12 degrees. The tide level at observation time is .8 meters. The majority of waves (80%) are predicted breaking at the offshore bar due to the wave height increase, resulting in additional dissipation. Some waves continue to break shoreward of the bar until reaching saturation at approximately 25 meters offshore where all waves break. Note how the bathymetric trough has widened by approximately 20 meters since 10 October, and beach slope has decreased. By October 14, smaller waves are arriving at an average period of 10 seconds and average incident angle of 7 degrees. At a low tide level of -.2 meters at

observation time, saturation occurs seaward of the bar. The dissipation region has narrowed and fewer waves reform in the trough, now widened by the storm to 50 meters. Beach slope has further decreased shoreward of the bar.

Using data acquired at 5 beaches, *Sallenger and Holman,* [1984] applied linear regression to conclude that for saturated breaking waves, γ is related to beach slope, β, (Fig 9) by the relation

$$\gamma_{rms} = 3.2\tan\beta + 0.30 \tag{22}$$

and that γ does not appear to depend on wave steepness. Optimal γ and σ values reflect wave and beach conditions (Table 1) and confirm the linear relationship in Equation (22). How these free parameters reflect changing conditions can be best observed during DELILAH. On October 10th, beach slope is steepest requiring a relatively large γ. On 12 October, larger waves have decreased the beach slope, reflected in the γ decrease. Finally, by 14 October the beach slope has decreased significantly resulting in a major decrease in γ.

Roller steepness, $\sin\sigma$, also changes with wave conditions; the steepest angles are required for plunging breakers, such as those occurring on the 12th, and smaller angles for spilling breakers. The same trends hold for the near-planar Leadbetter and Torrey Pines beaches, but with smaller percent rms error due to constant beach slopes.

V. DISCUSSION AND CONCLUSIONS

Sensitivity tests varying σ and γ versus rms wave height prediction error are shown in Figures 10a and 10b. All model runs, regardless of wave or beach conditions, produce the same trends. Roller steepness can vary up to 40 degrees in most cases negligibly changing rms error. The reason for insensitivity to σ is seen by examining the energy flux balance Equation (16).

Roller steepness is used to describe both the surface roller production and dissipation terms. After substituting $\tan\sigma$ into Equation (10) into the dissipation term Equation (12), $\tan\sigma$ cancels and remains only in the roller energy term. As shown in Figures 2b-8b, the gradient wave energy flux is more than two orders of magnitude larger than the gradient roller energy flux term. This effectively reduces the surface roller model free parameters from two to one in γ.

The model is sensitive to changes in gamma. The expected range of γ using Equation (22) is .3 to .6 for the range of beach slopes from 0-.1. Examples of varying gamma for planar and barred beaches are shown in Figure 11b. Model error is fairly insensitive for the barred beach (±2%) when gamma is within the range .3 to .5. Error rapidly increases for gamma outside this range. The reason for the rate of change difference can be seen analyzing small and large gammas in Equation (16). As rms wave height is raised to the 5th power in the roller energy and dissipation terms compared with the 2nd power as in the wave energy term, a small decrease in γ causes the magnitude of the gradient roller energy flux and dissipation terms to rapidly approach wave energy flux magnitude. This rapid change in magnitude causes rapid changes in rms wave height prediction and percent rms error. A large positive change in γ only decreases the roller energy and dissipation terms more, which are already small relative to the wave term, resulting in slower percent rms error rate changes.

Relatively low values of γ compared to the expected range (.3-.6) are required to minimize the rms error for Torrey Pines data (Table 1). The reason is hypothesized to be linear bore theory deficiencies

based on conclusions by *Cacina,* [1989]. A review of the bore dissipation model is required for further investigation.

The bore dissipation model [*Thornton and Guza,* 1983] predicts shoreward rms wave heights within an rms error of ±9% for random waves and arbitrary bottom profiles using the same data for Torrey Pines and Leadbetter Beaches. The bore model energy flux balance equation is given by Equation (3), D being described by linear bore dissipation. Frictional dissipation at the bottom boundary layer is shown to be negligible (less than 3% of breaking wave dissipation within the surf zone) except in the run-up region and it is subsequently neglected.

Applying conservation of mass and momentum at regions of flow upstream and downstream of the bore, the average rate of energy dissipation per unit area is calculated [*Stoker,* 1957]

$$\epsilon_b = \frac{1}{4}\rho g \frac{(h_2 - h_1)^3}{h_1 h_2} Q = \frac{1}{4}\rho g \frac{(BH)^3}{h^2} Q \tag{23}$$

where B is a breaker coefficient of O(1), representing the fraction of foam on the wave face (accounts for various breaker types). Q is the volume discharge per unit area across the bore (Fig 11), described simplest by *Hwang and Divoky,* [1970] as

$$Q = \frac{Ch}{L} \tag{24}$$

where C is wave speed and L wavelength. Substitution into Equation (23) yields

$$\epsilon_b = \frac{\rho g (BH)^3 C}{4Lh} = \frac{\rho g \bar{f} (BH)^3}{4h} \qquad (25)$$

The bore dissipation function has the same form as roller dissipation with the exception of the B coefficient. The reason for their similarity is because a hydraulic jump (or bore) is used to calculate the area of a roller (Equation 10) when deriving roller dissipation. The fact that they both are similar after derivation from two perspectives would lead one to expect similar results.

The surface roller model differs from the bore dissipation model by only the roller energy term. Although the roller term is much smaller than the wave energy term, it is a significant addition to the bore model. The term provides two changes. First, it allows the propagation of dissipation shoreward. Bore model dissipation results for 12 October (DELILAH) and 4 February at Santa Barbara (Fig 12) are compared with the roller model (Figs 3a and 5a). The dissipation plots are similar for both models at the planar beach, and in the offshore bar region at Duck. The significant difference occurs in the trough at the barred beach. In the bore model, waves stop breaking in the trough moving dissipation towards zero. In the roller model, waves break at the offshore bar and the roller continues through the trough and nearshore region, which is more in line with observations. The net result is the roller model more accurately predicts shoreward wave heights while providing more accurate offshore dissipation values, as shown by the numerical scheme in Equation (21).

Secondly, the roller model decreases the number of sensitive input parameters. *Thornton and Guza,* [1983] conclude simple bore theory underestimates dissipation, for which the B parameter compensates. They also conclude that B and γ could be combined into one coefficient, but are left separate for greater physical insight. *Cacina,* [1989] combined the B and γ term, called the BG parameter, described by

$$BG = \frac{B^3}{\gamma^2} \tag{26}$$

The bore dissipation model was iterated over the BG parameter to reduce percent rms error in a least squares sense. Results of one barred beach day are shown in Figure 13, revealing a similar free parameter/rms error curve as the roller model.

Cacina, [1989] concluded that B, a measure of wave breaking intensity, is correlated with the deep water surf similarity parameter described by Equation (1). It should follow that the roller model's single sensitive free parameter, γ, be a function of beach slope and the deep water surf similarity parameter. Results of varying γ with these parameters for all days over various bottom profiles are shown in Figures 14-16 and Table 1. An approximate linear relationship exists between γ, $\tan\beta$, and ζ, confirming previous conclusions by *Battjes* [1974], and *Sallenger and Holman* [1984]. A high correlation coefficient of 0.93 is found between γ and $\tan\beta$ (Fig 14). Gamma is not as highly correlated (.67) with wave steepness (H_0/L_0) (Fig 15) or the deep water surf similarity parameter (.58) (Fig 16) .

Roller model accuracy may be improved by using variable coefficients across the surf zone. Constant γ's and σ's were used for each run. Optimal values were chosen by fitting model generated H_{rms} values to observed wave heights. Improvement would require γ and σ be specified throughout the wave prediction region.

In applying the model based on this analysis, using γ=.31 gives wave height prediction accuracy within 10% rms error for all beach profiles. For barred beaches, a value of γ=.34 is suggested; for planar beaches, use γ=.30 (averages for barred and planar beach days). σ=20 degrees is sufficiently accurate for all profiles. The lower than expected values of γ according to Equation (22) indicates that the roller model γ is accounting for other factors associated with complex wave breaking processes.

The roller model improves the bore model by decreasing average rms error from 8.6% to 4.5% for all breaker types and variable bathymetry, accomplished by more accurately describing dissipation throughout the surf zone. The roller model simultaneously reduces the requirement of two free parameters to essentially one in γ.

REFERENCES

Basco, D.R., A Qualitative Description of Wave Breaking, Submitted to *Journal of Waterway, Port, Coastal and Ocean Engineering*, American Society of Coastal Engineering, July 1983.

Battjes, J.A., Surf Similarity, *Proceedings of the 14th International Conference Coastal Engineering*, American Society of Civil Engineers, 466-480, New York, 1978.

Battjes, J.A., and J.P.F.M. Janssen, Energy loss and set-up due to breaking of random waves, *Proceedings of the 16th International Conference Coastal Engineering, 589*, American Society of Civil Engineers, New York, 1978.

Bradshaw, P. and Ferris, D.H., The spectral energy balance in a turbulent mixing layer, *Report 1144*, National Physical Laboratory, Aerodynamics Division, 1965.

Cacina, N., Test and Evaluation of Surf Forecasting Model, *M.S. Thesis*, Naval Postgraduate School, Monterey, 1989.

Church, C. and E.B. Thornton, Effects of Breaking Wave Induced Turbulence within a longshore current model, *J. Coastal Engineering* (in press), 1993.

Engelund, F., A simple theory of weak hydraulic jumps, *Progress Report No. 54, Institute of Hydrodynamics and Hydraulic Engineering, ISVA*, Technical University Denmark, 29-32, 1981.

Fredsoe, J. and R. Deigaard, Mechanics Of Coastal Sediment Transport, *Advanced Series on Ocean Engineering, 3*, 103, 1992.

Hwang, L.S. and D. Divosky, Breaking Wave Setup and Decay on Gentle Slopes, *Proceedings of the 12th International Coastal Engineering Conference, American Society Of Civil Engineers*, New York, 377-389, 1970.

Pawka, S.S., D.L. Inman, R.L. Lowe, and L. Holmes, Wave climate at Torrey Pines Beach, Calif., *Tech. Pap. 76-5*, Coastal Eng. Res. Center, Fort Belvoir, Va., 1976.

Sallenger, A.H. and Robert A. Holman, Wave-Energy saturation on a natural beach of variable slope, paper not yet published, U.S. Geological Survey and Oregon State University, 1984.

Svendsen, I.A. and Madsen, P.A., A turbulent bore on a beach, *J. Fluid Mechanics, 148*, 73-96, 1984.

Svendsen, I.A., Wave Heights and set-up in a surf zone, *Coastal Engineering, 8(4)*, 303-329, 1984.

Stoker, J.J., *Water Waves*, Interscience, New York, 1957.

Thornton, E.B. and R.T. Guza, Transformation of wave height distribution, *J. Geophysical Res., 88(c10)*, 5925-5938, 1983.

Thornton, E.B. and R.T. Guza, Surf zone longshore currents and random waves: Field data and models, *J. Physical Oceanogr.*, *16*, 1165-1178, 1986.

TABLE 1. ROLLER MODEL PARAMETER RESULTS. Free parameter values are given with resulting predicted vs observed wave height rms error. 1. Beach slope- mean slopes for planar beach days; foreshore slopes for barred beach days. 2. Mean incident wave frequency in Hertz. 3. Deep water wave steepness parameter.4. Deep water surf similarity parameter. 5. Mean incident wave angle in degrees. 6. The number of wave height observations for a given day. 7. Roller steepness angle- an adjustable free parameter in the roller model. 8. Gamma- an adjustable free parameter in the roller model. 9. Percent root mean squared error for observed vs model predicted wave heights.

DATE	$\tan\beta$[1]	f (Hz)[2]	H_o/L_o[3]	ζ_o[4]	α[5]	#obs[6]	σ[7]	γ[8]	%Error[9]
10Oct	.053	.103	.0055	.719	1.9	07	30	.37	4.7
12Oct	.042	.064	.0027	.808	11.3	06	40	.34	5.1
14Oct	.040	.103	.0049	.582	6.5	08	30	.30	9.7
04Feb	.038	.070	.0024	.875	9.0	13	5	.32	2.6
05Feb	.035	.078	.0023	.801	8.4	10	20	.32	2.5
04Nov	.021	.070	.0010	.662	0.0	12	10	.28	3.7
10Nov	.021	.063	.0014	.572	0.0	11	15	.27	3.1
All days						67	21	.31	4.5

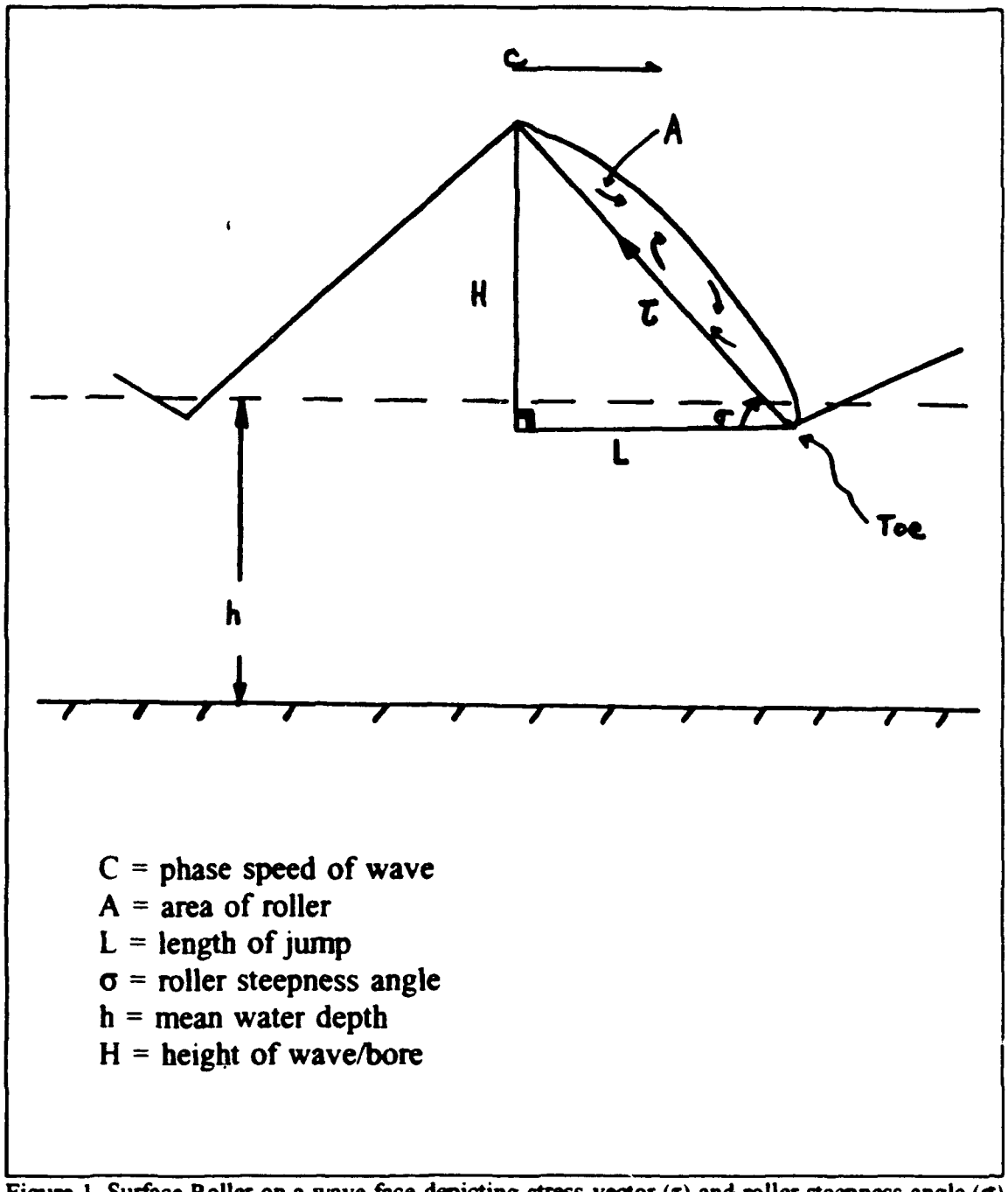

Figure 1. Surface Roller on a wave face depicting stress vector (τ) and roller steepness angle (σ) with respect to horizontal.

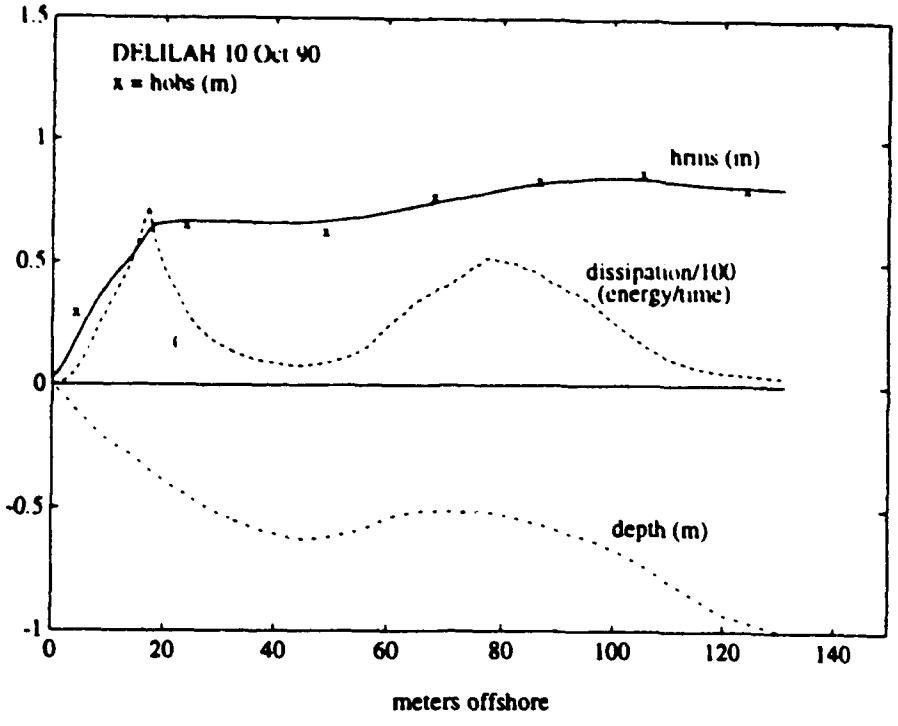

Figure 2a. Roller model wave height prediction using γ=.37, σ=30 degrees.

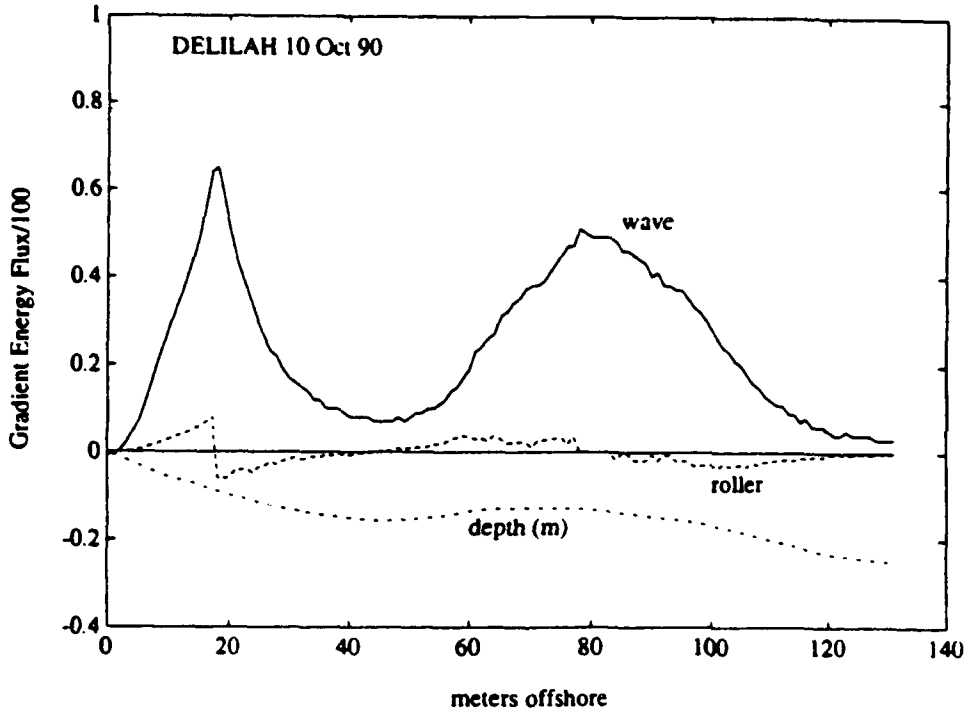

Figure 2b. Roller model gradient wave and gradient roller energy flux. γ=.37, σ=30 degrees.

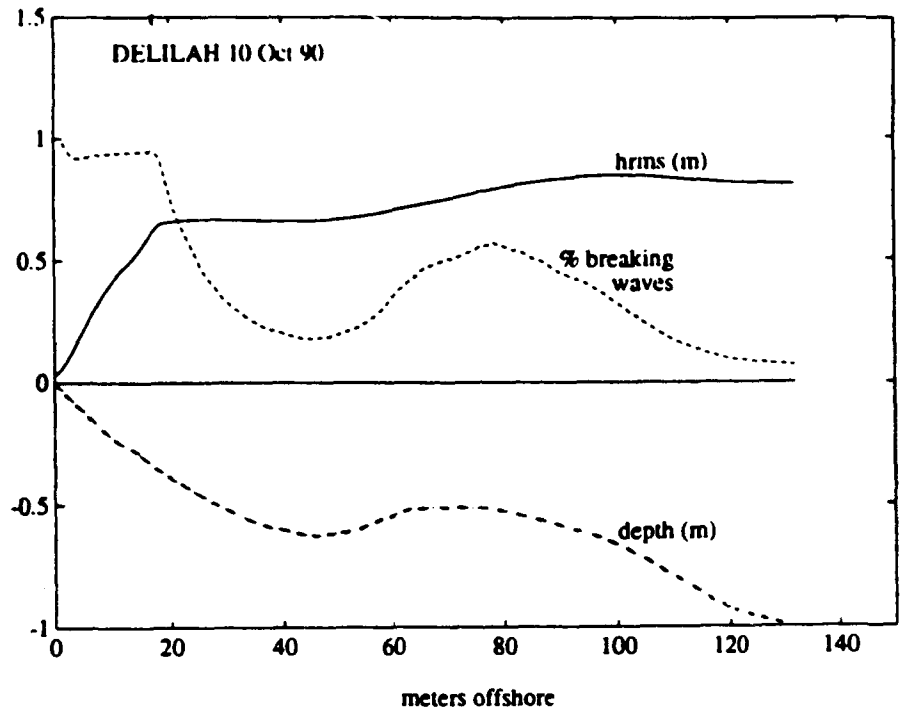

Figure 2c. Percent of waves breaking as a function of offshore distance and depth.

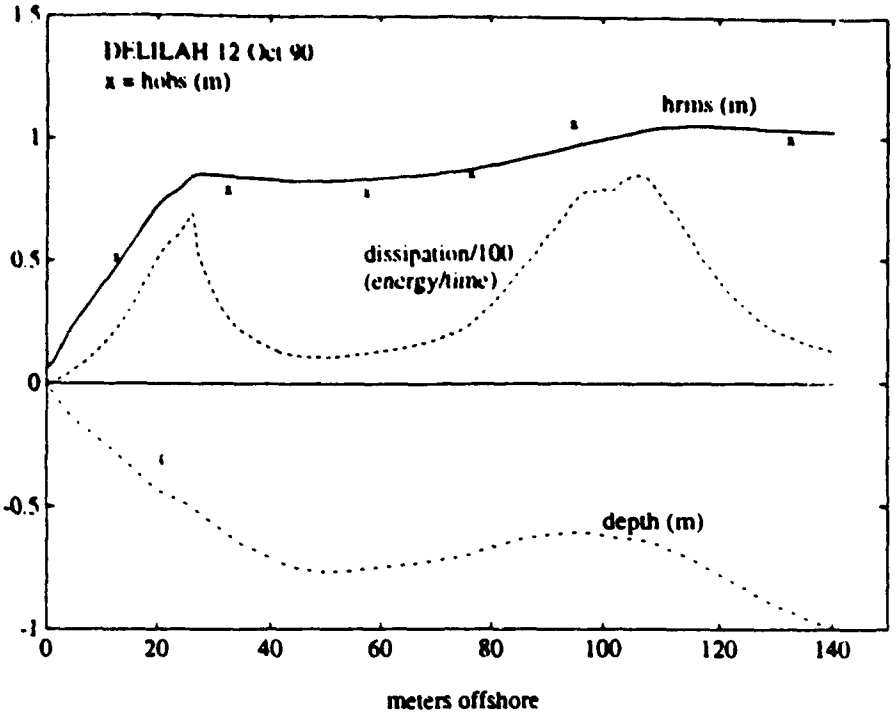

Figure 3a. Roller model wave height prediction using γ=.34, σ=40 degrees.

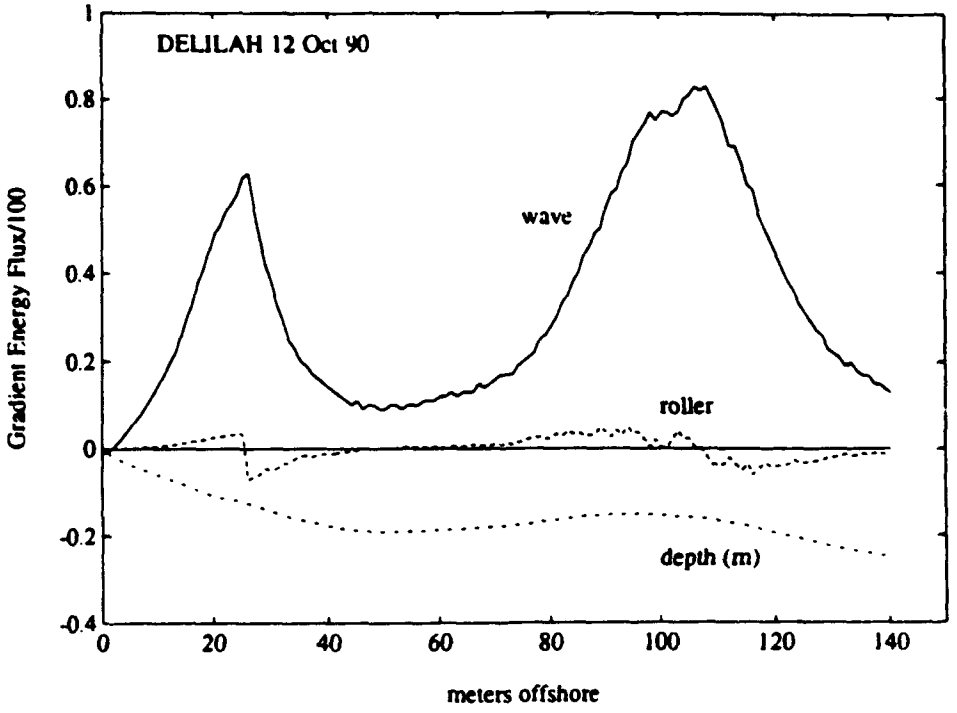

Figure 3b. Roller model gradient wave and gradient roller energy flux. γ=.34, σ=40 degrees.

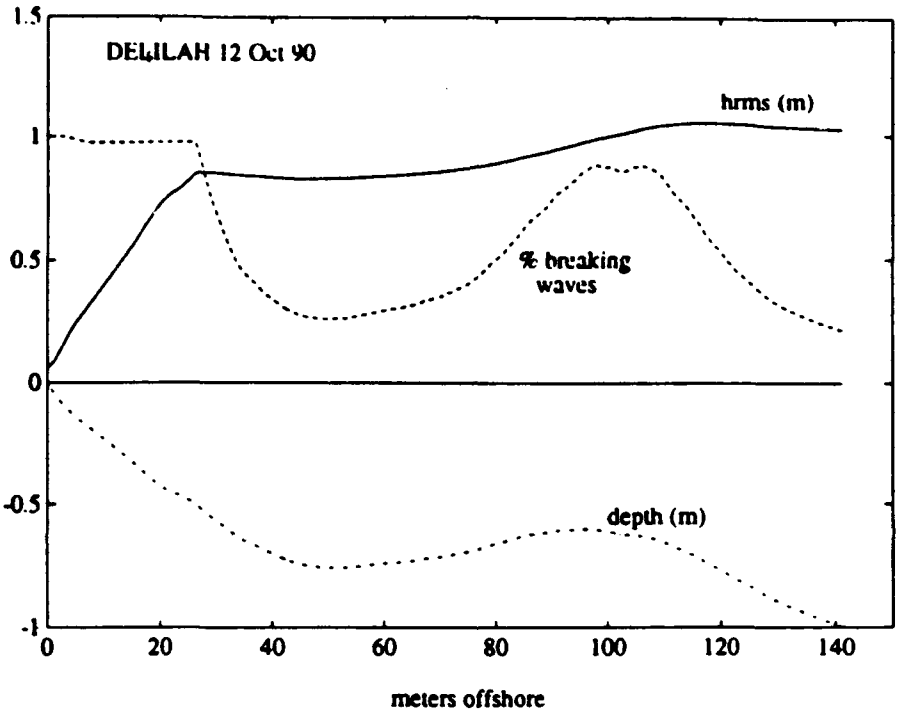

Figure 3c. Percent of waves breaking as a function of offshore distance and depth.

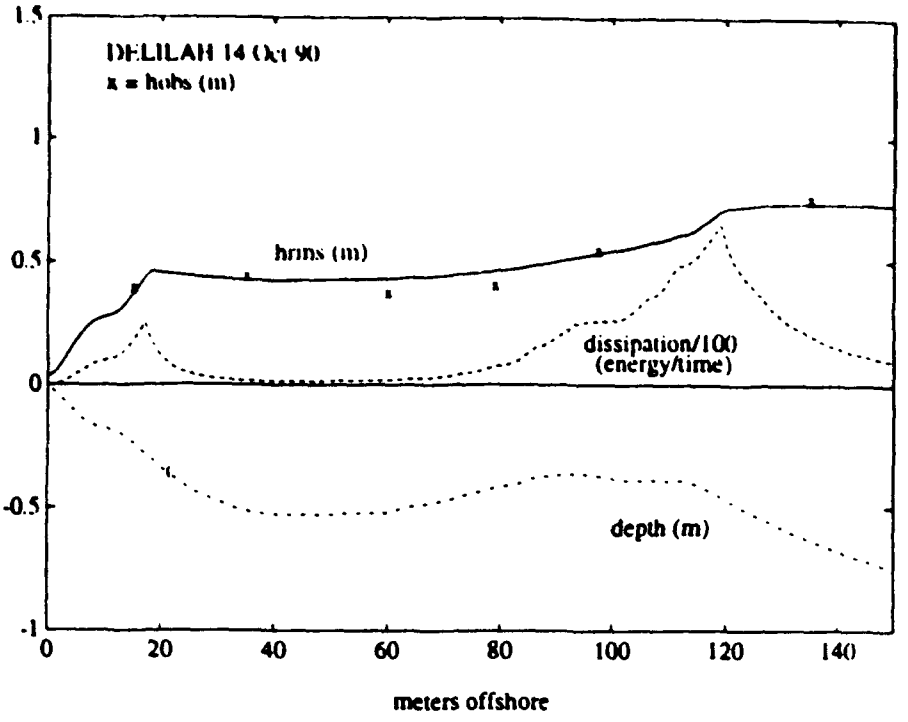

Figure 4a. Roller model wave height prediction using γ=.30, σ=30 degrees.

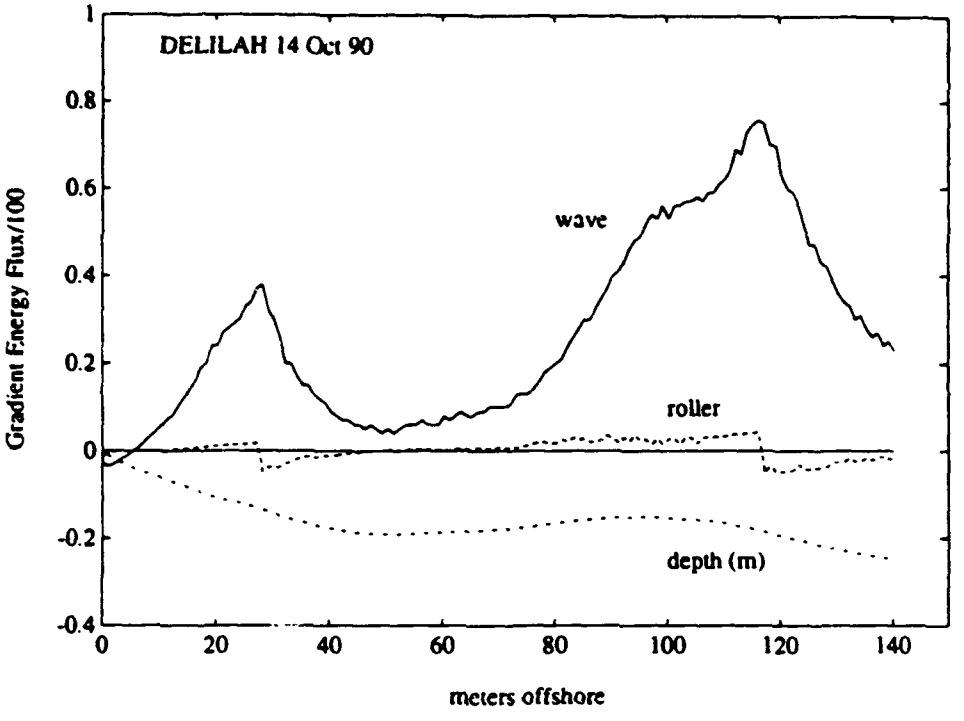

Figure 4b. Roller model gradient wave and gradient roller energy flux. γ=.30, σ=30 degrees.

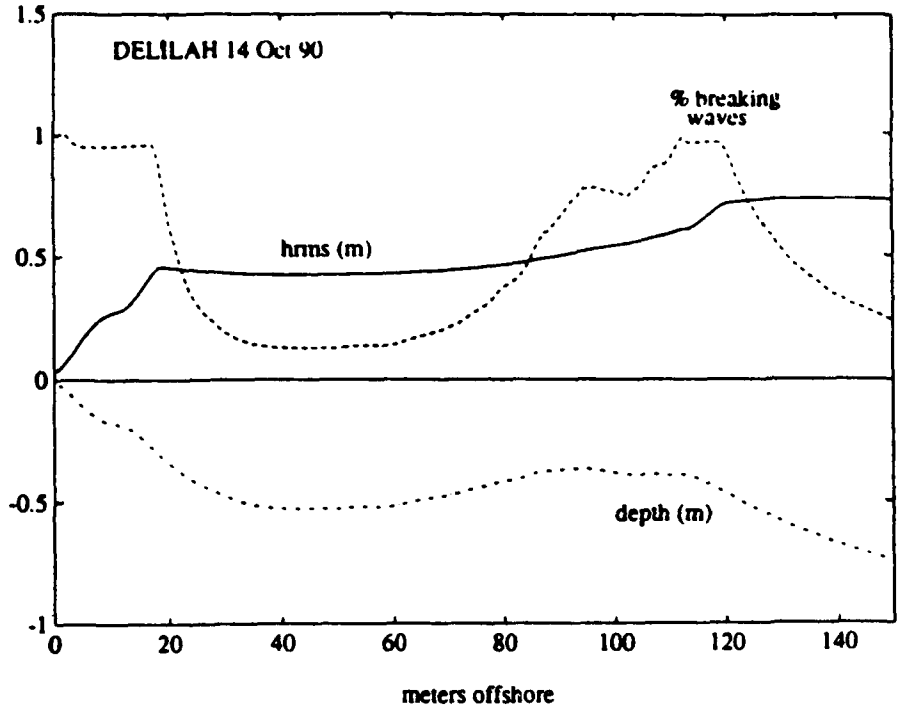

Figure 4c. Percent of waves breaking as a function of offshore distance and depth.

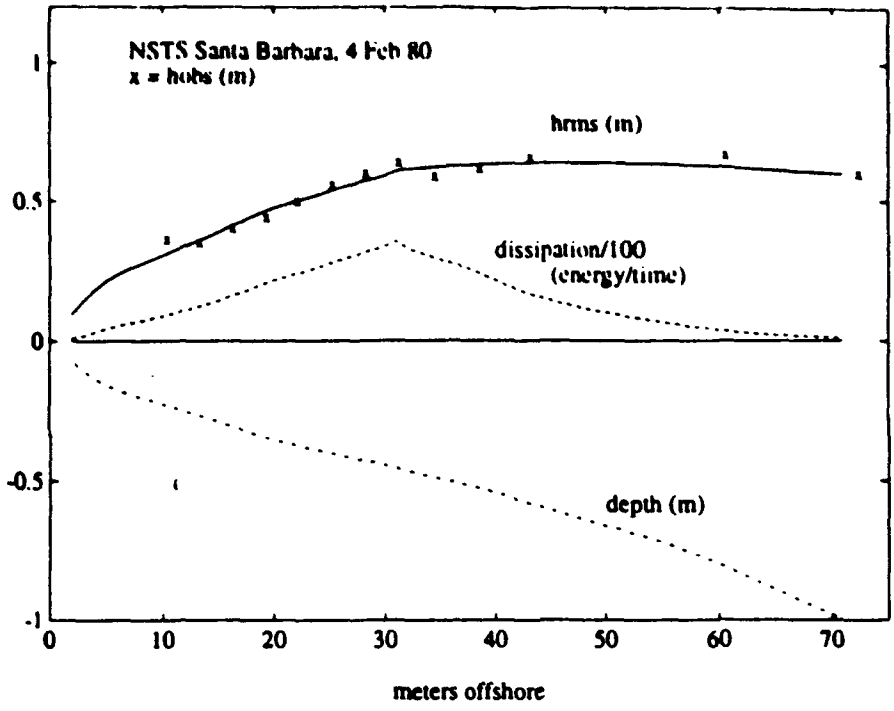

Figure 5a. Roller model wave height prediction using γ=.32, σ=5 degrees.

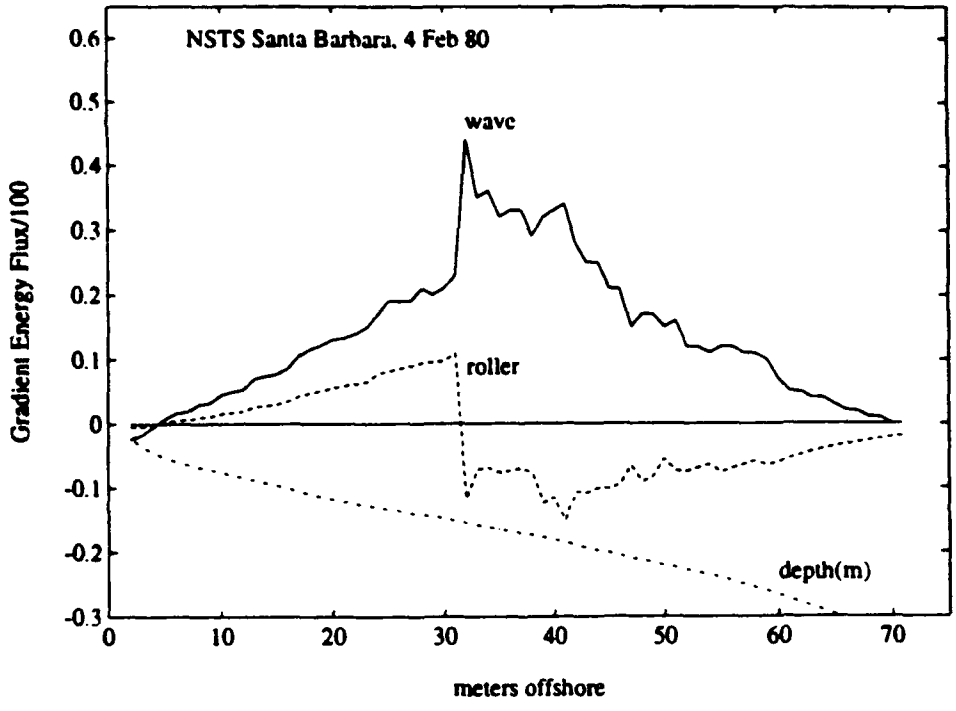

Figure 5b. Roller model gradient wave and gradient roller energy flux. γ=.32, σ=5 degrees.

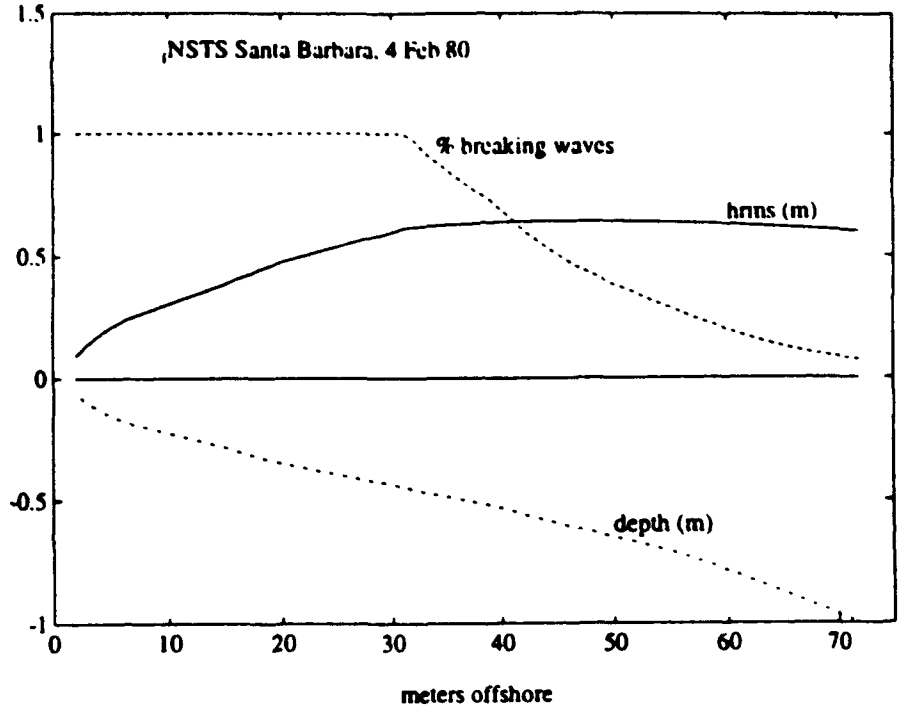

Figure 5c. Percent of waves breaking as a function of offshore distance and depth.

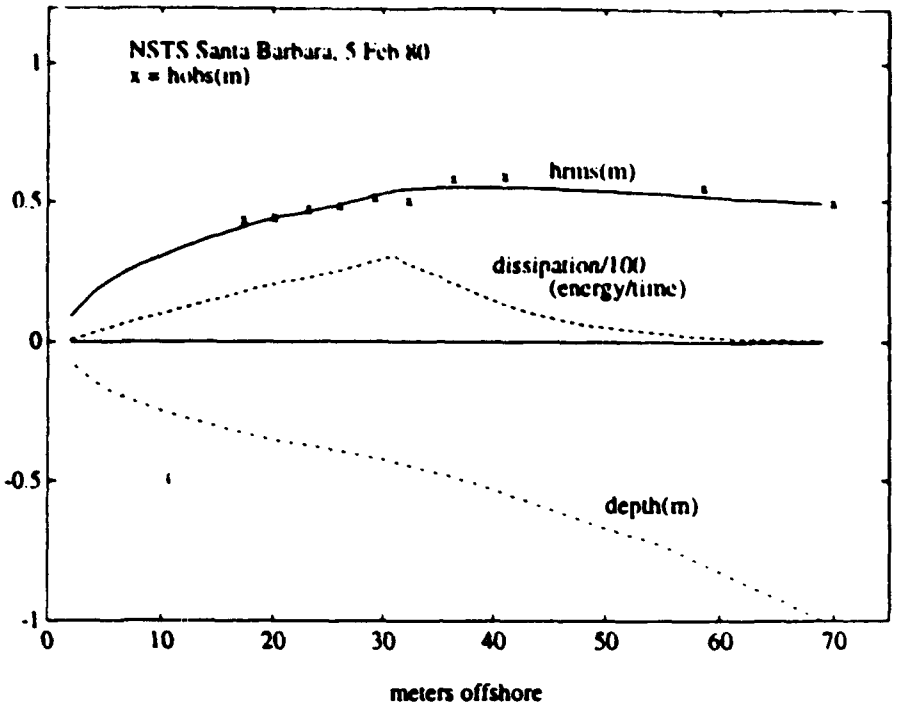

Figure 6a. Roller model wave height prediction using γ=.32, σ=20 degrees.

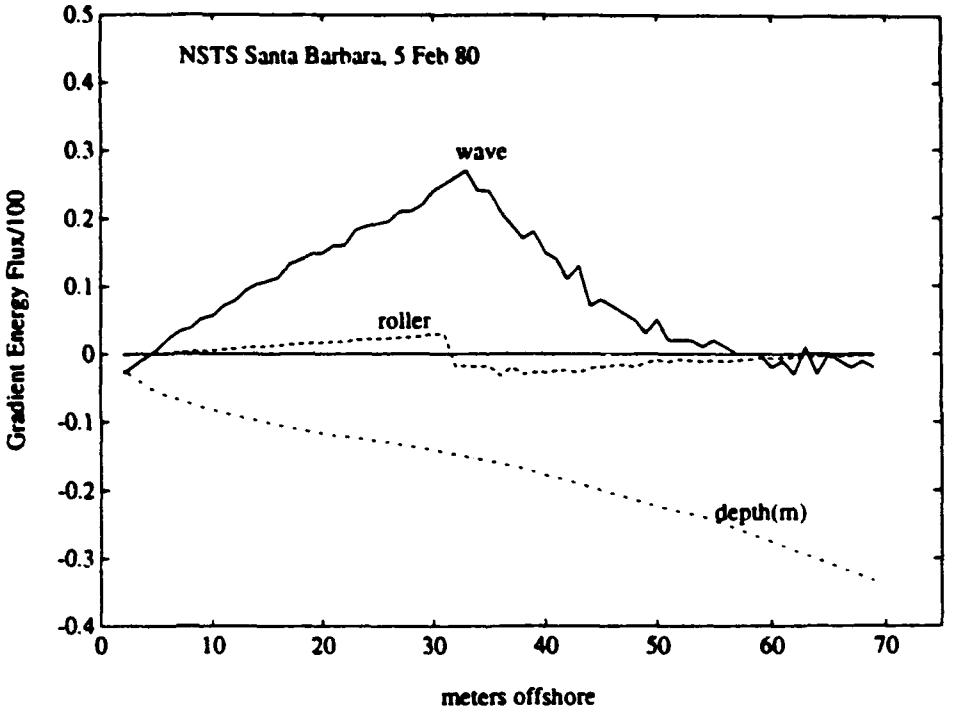

Figure 6b. Roller model gradient wave and gradient roller energy flux. γ=.32, σ=20 degrees.

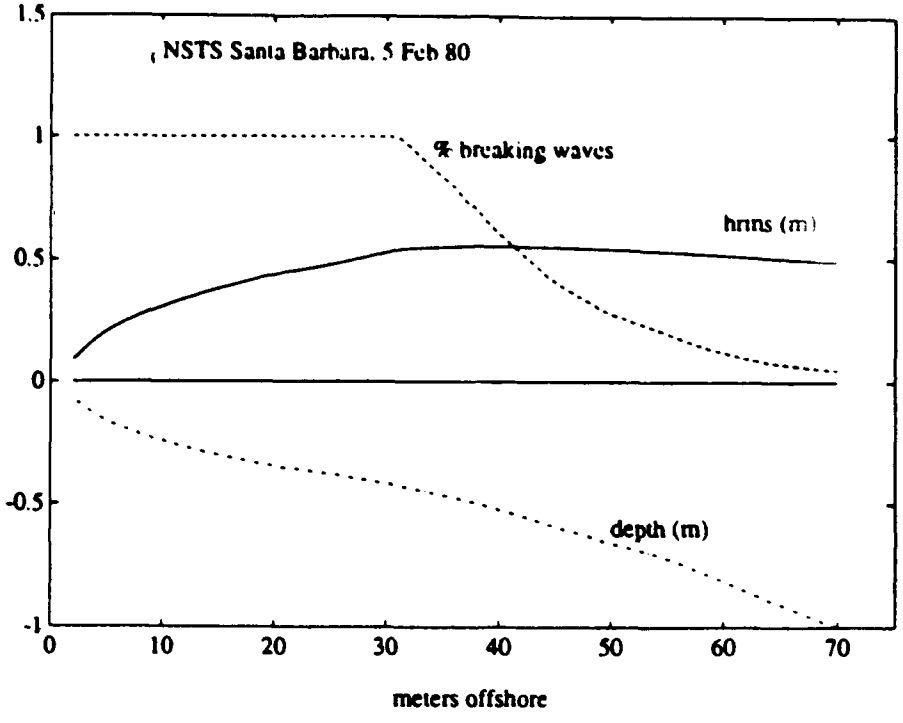

Figure 6c. Percent of waves breaking as a function of offshore distance and depth.

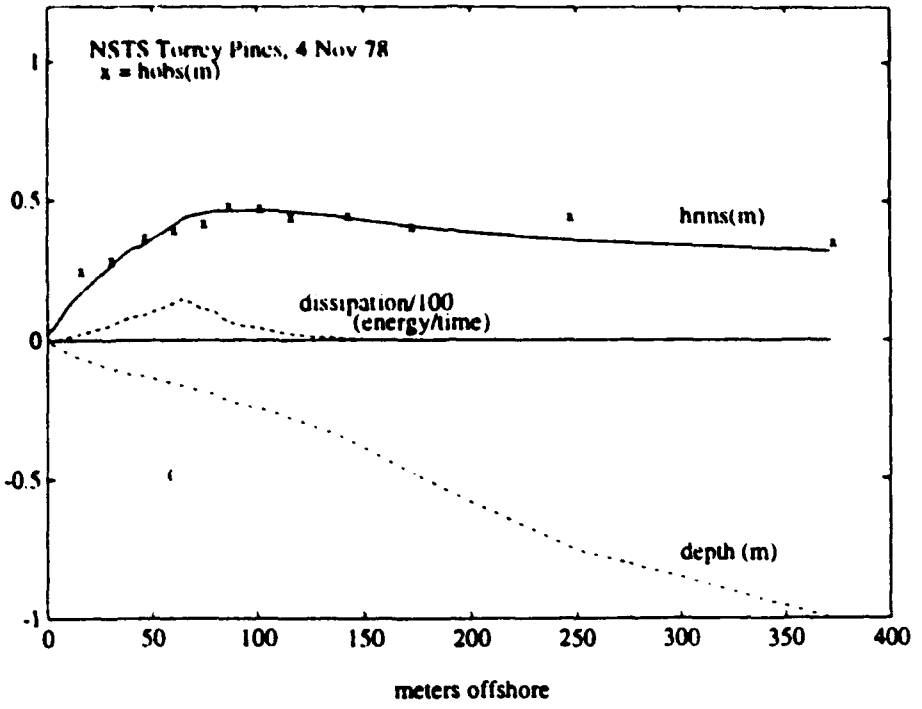

Figure 7a. Roller model wave height prediction using γ=.28, σ=10 degrees.

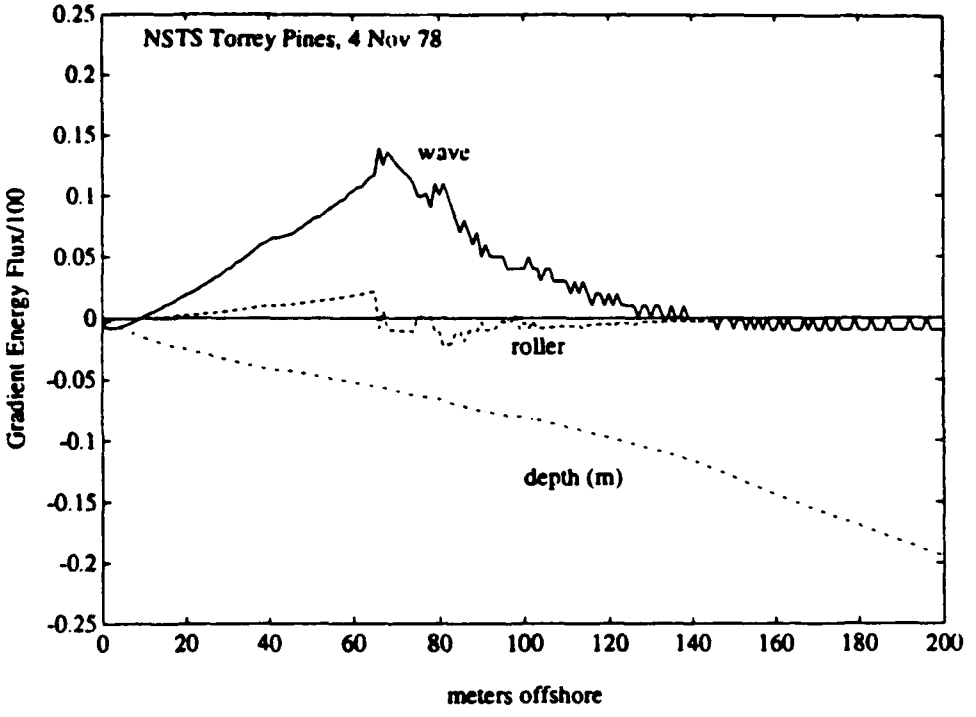

Figure 7b. Roller model gradient wave and gradient roller energy flux. γ=.28, σ=10 degrees.

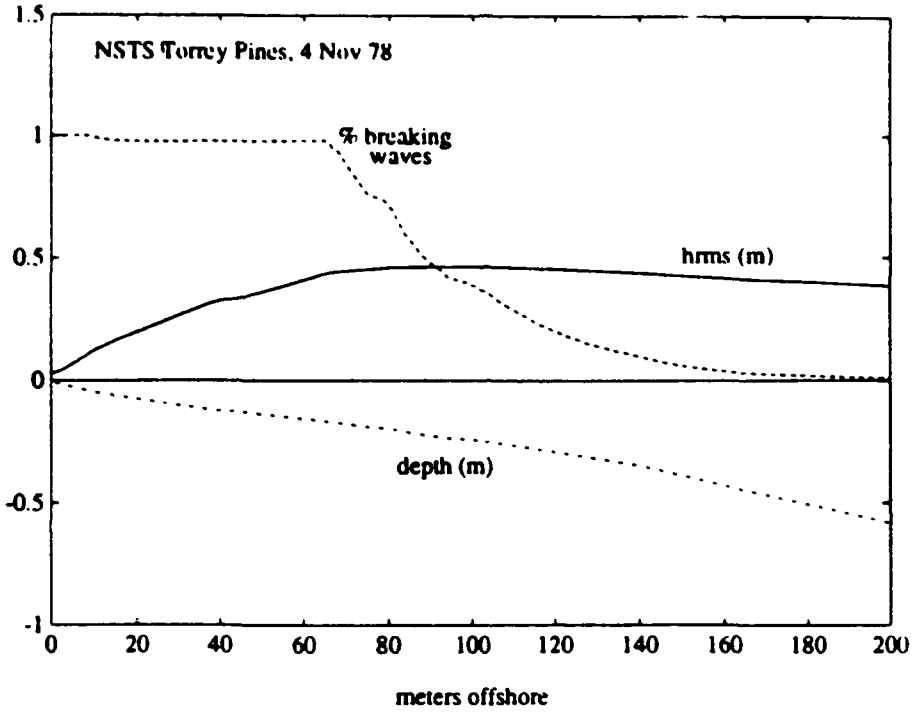

Figure 7c. Percent of waves breaking as a function of offshore distance and depth.

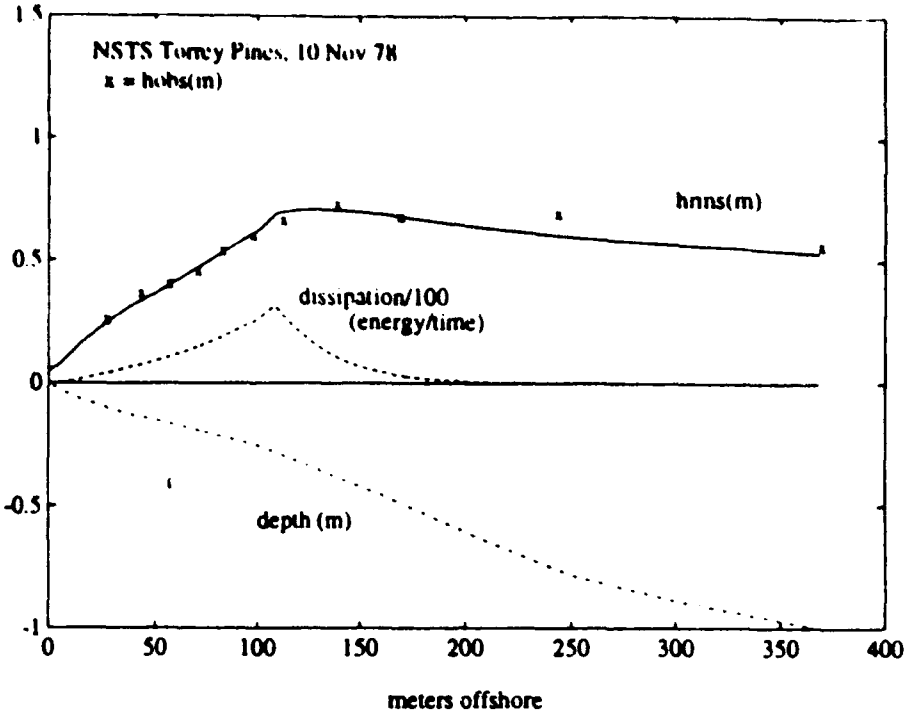

Figure 8a. Roller model wave height prediction using γ=.27, σ=15 degrees.

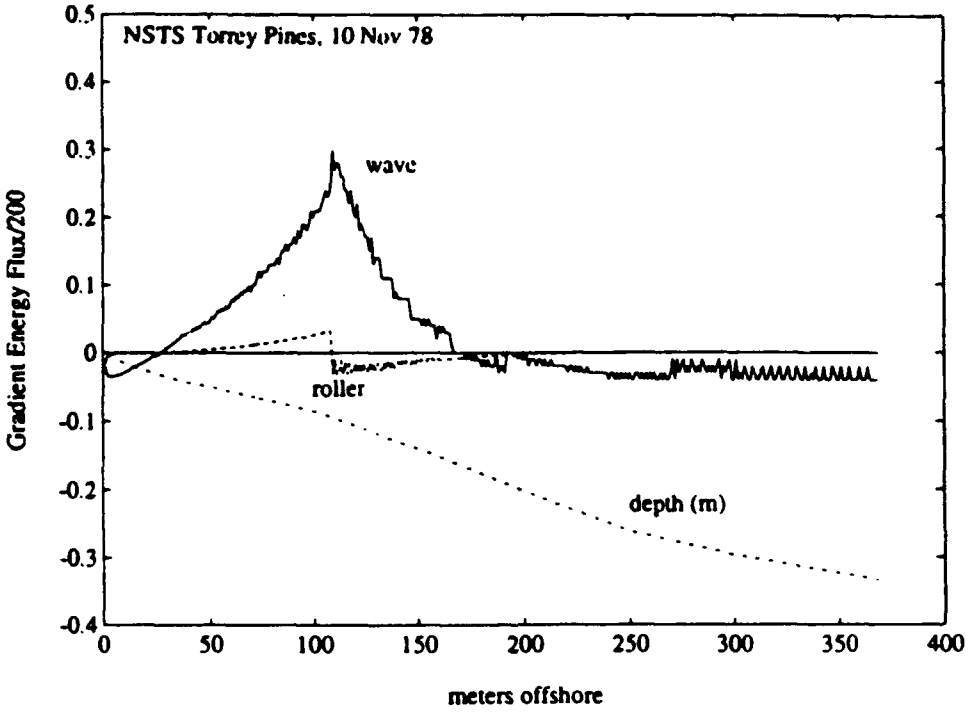

Figure 8b. Roller model gradient wave and gradient roller energy flux. γ=.27, σ=15 degrees.

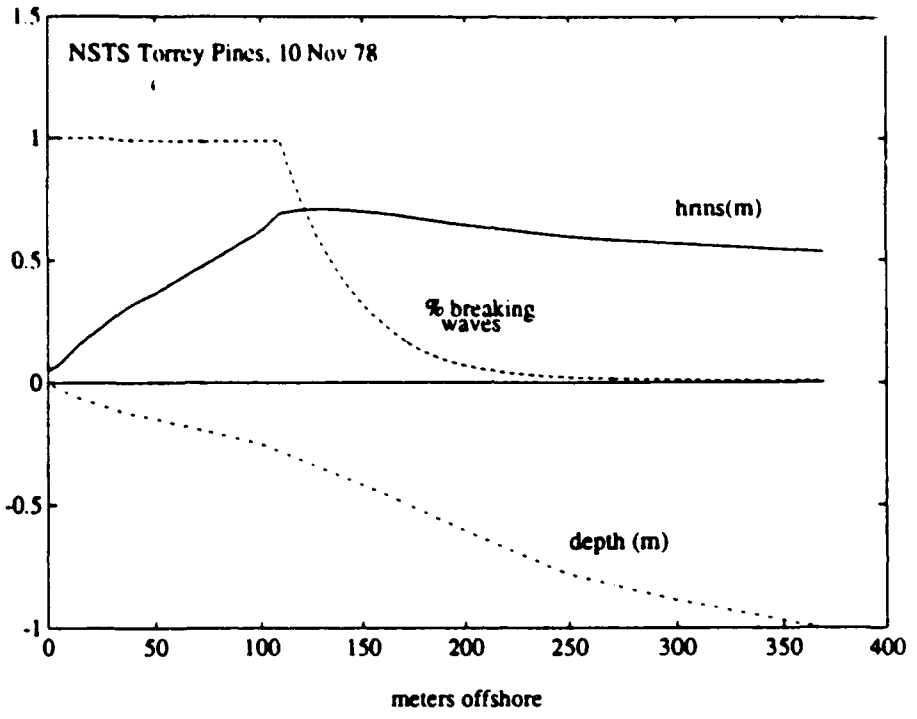

Figure 8c. Percent of waves breaking as a function of offshore distance and depth.

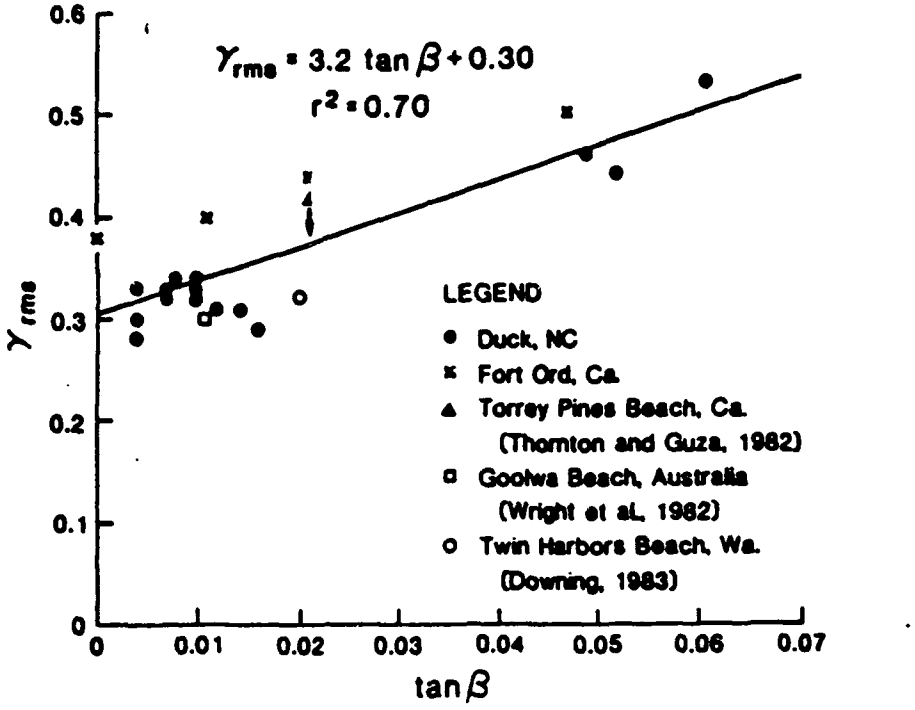

Figure 9. Gamma and beach slope relationship (*Sallenger and Holman*, 1984).

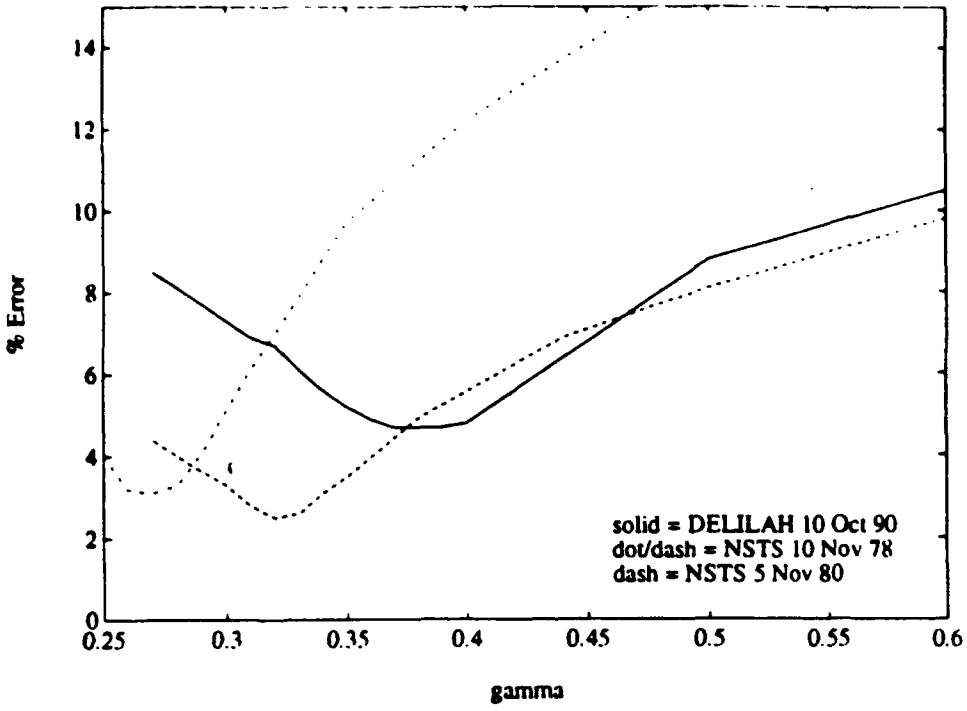

Figure 10a. Gamma sensitivity test using optimum σ's from Table 1.

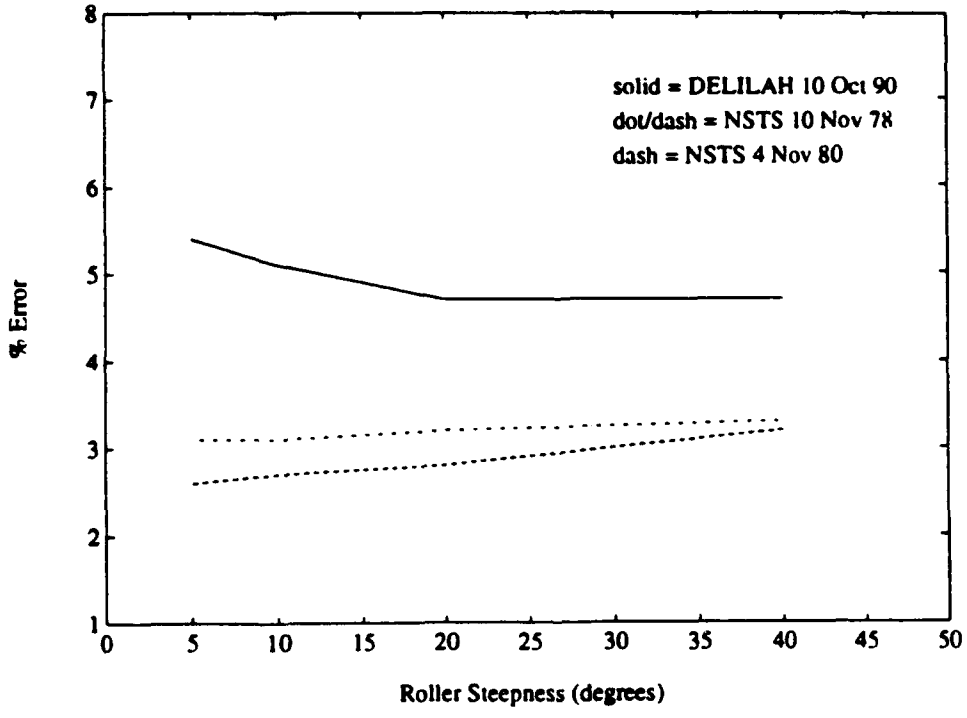

Figure 10b. Sigma sensitivity test using optimum γ's from Table 1.

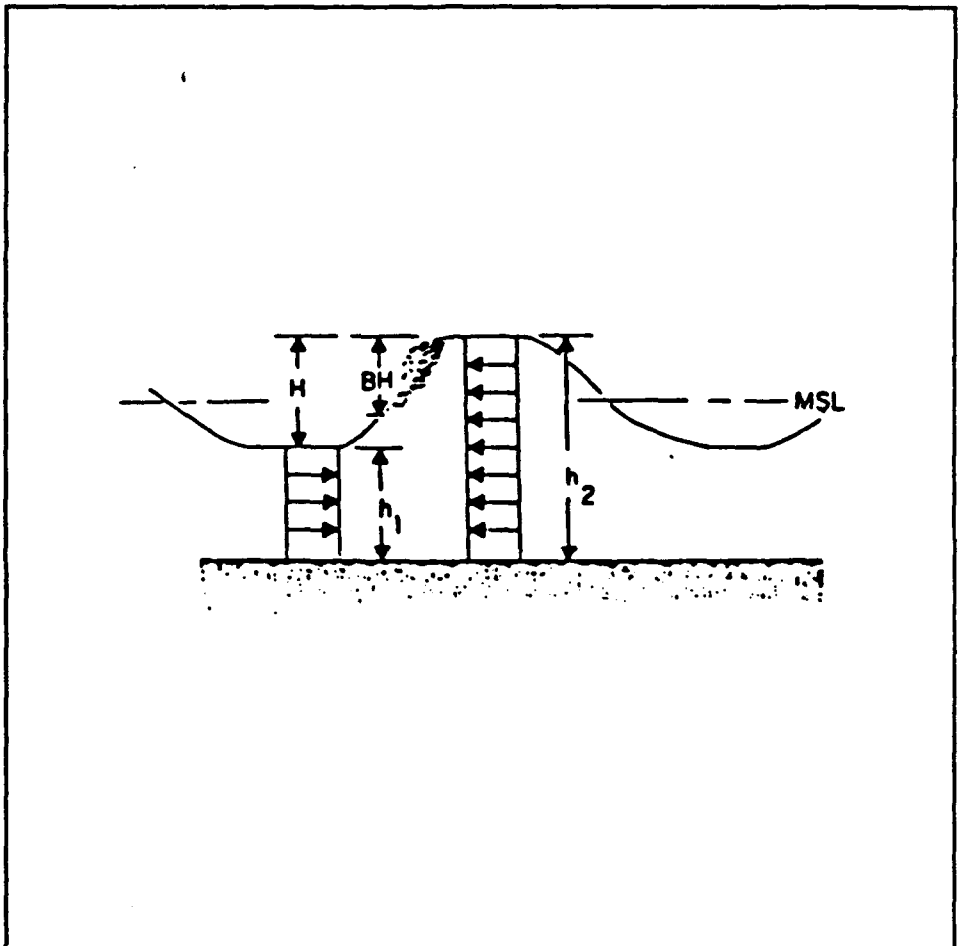

Figure 11. Periodic bore used to describe spilling breakers (from *Thornton and Guza*, 1983).

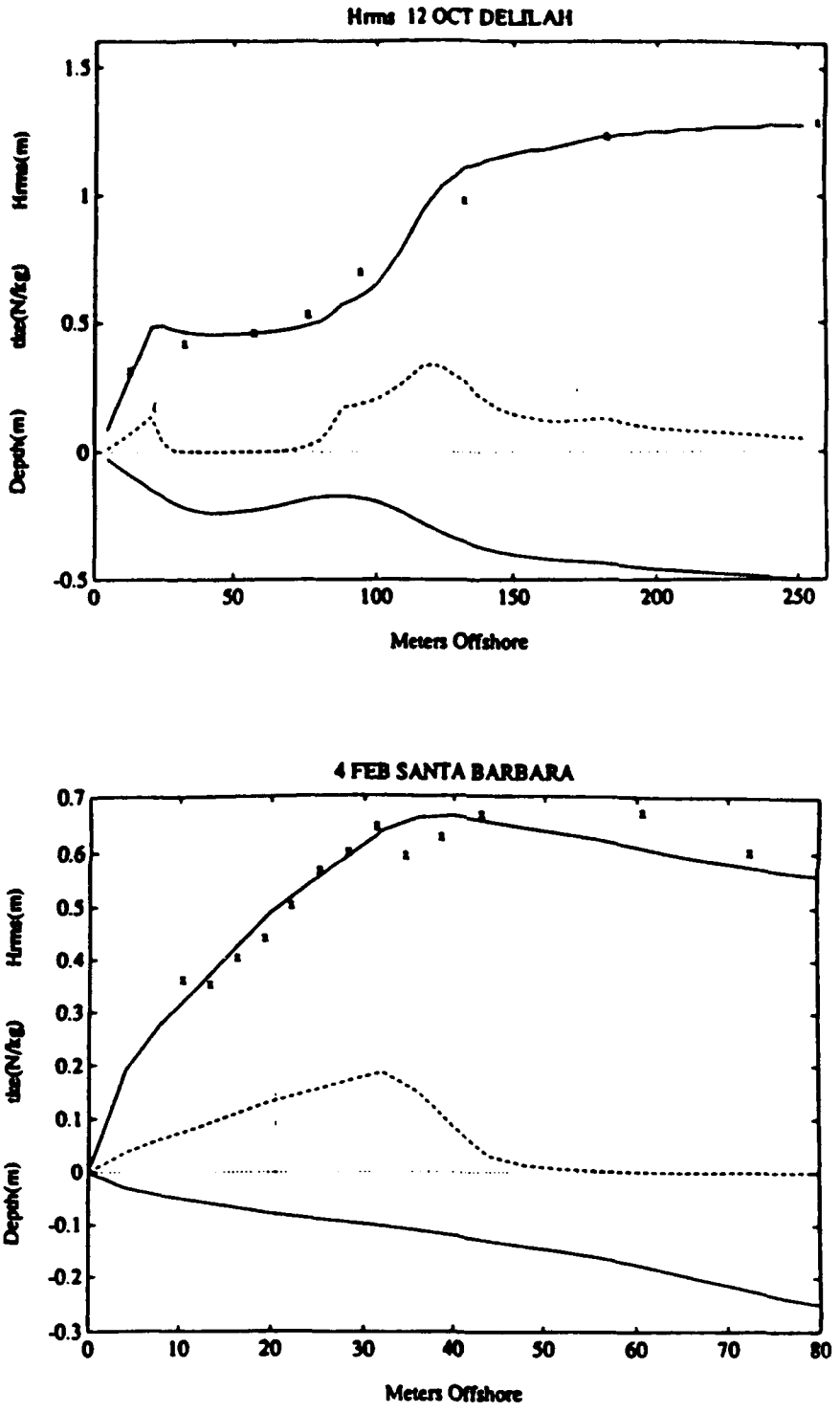

Figure 12. DELILAH experiment. Bore Model rms wave height prediction in meters (solid line above zero reference line), turbulent kinetic energy calculation or dissipation (dashed line), zero reference (dotted line), and depth in meters (solid line below zero reference) on days indicated (Church and Thornton, 1993).

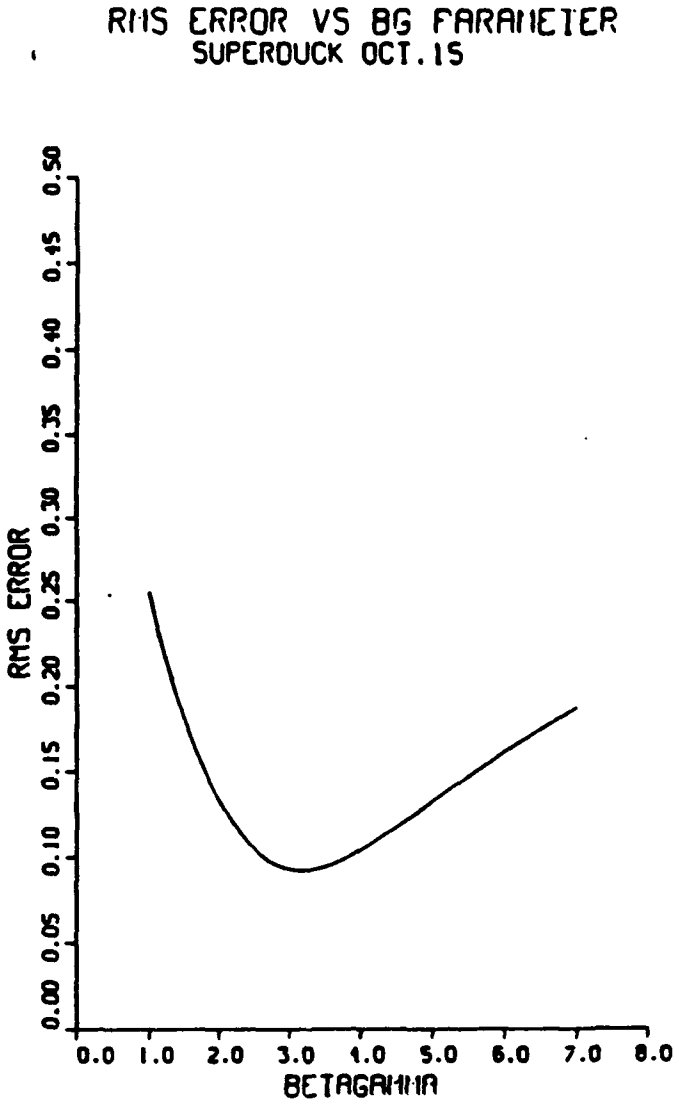

Figure 13. Variation in rms error due to change in BG parameter for a bore dissipation model run on a barred beach during SUPERDUCK experiment in Duck, N. Carolina (from *Cacina*, [1989]).

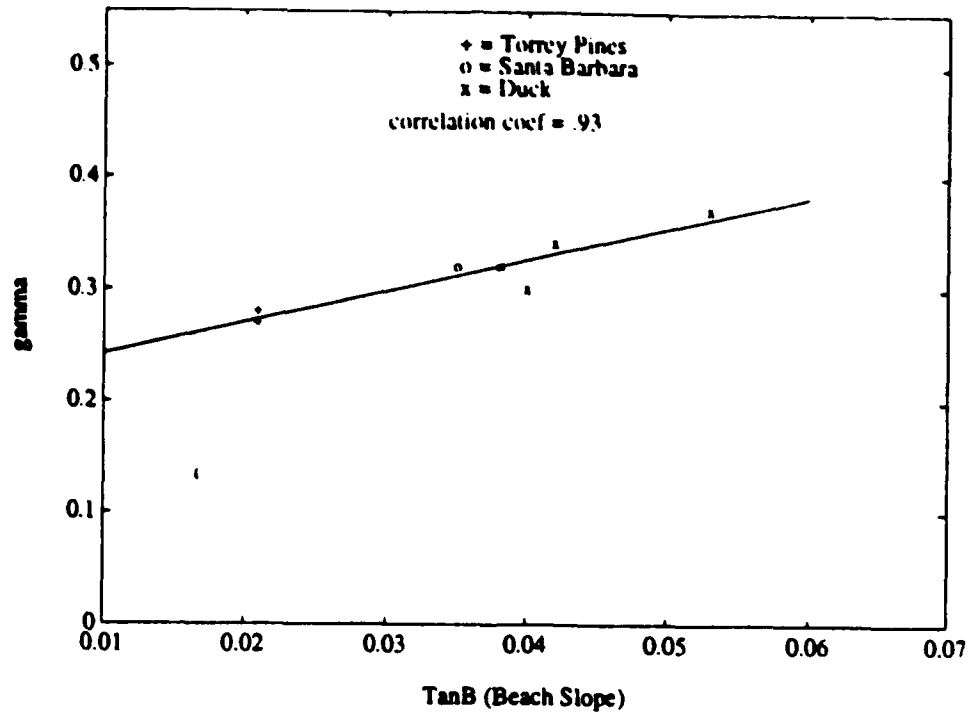

Figure 14. Correlation of γ and beach slope, $\tan\beta$.

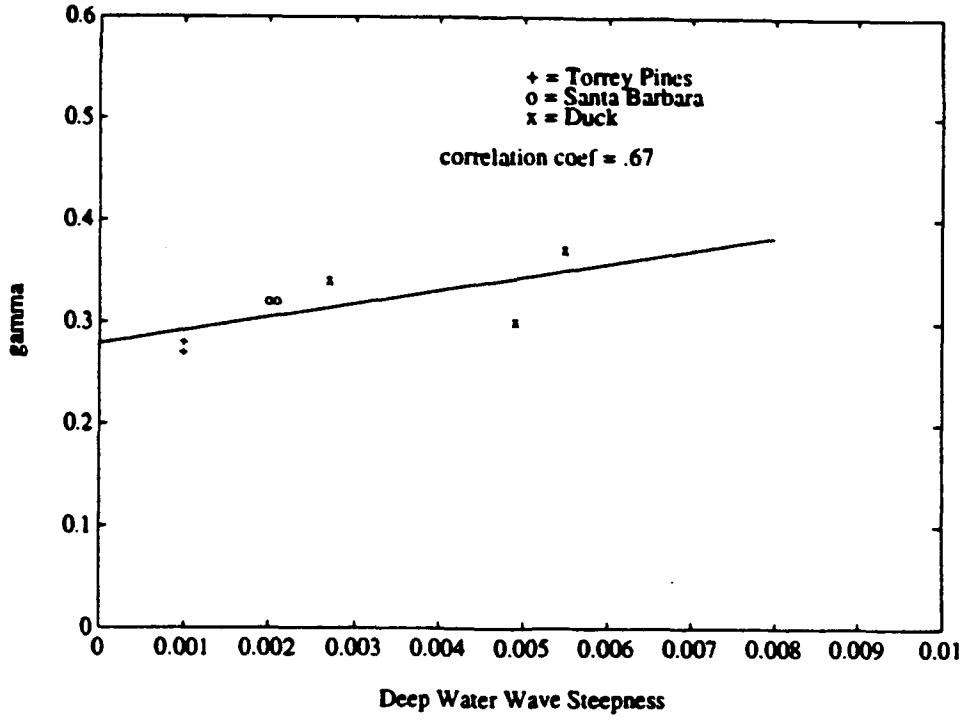

Figure 15. Correlation of γ and deep water wave steepness (H_o/L_o).

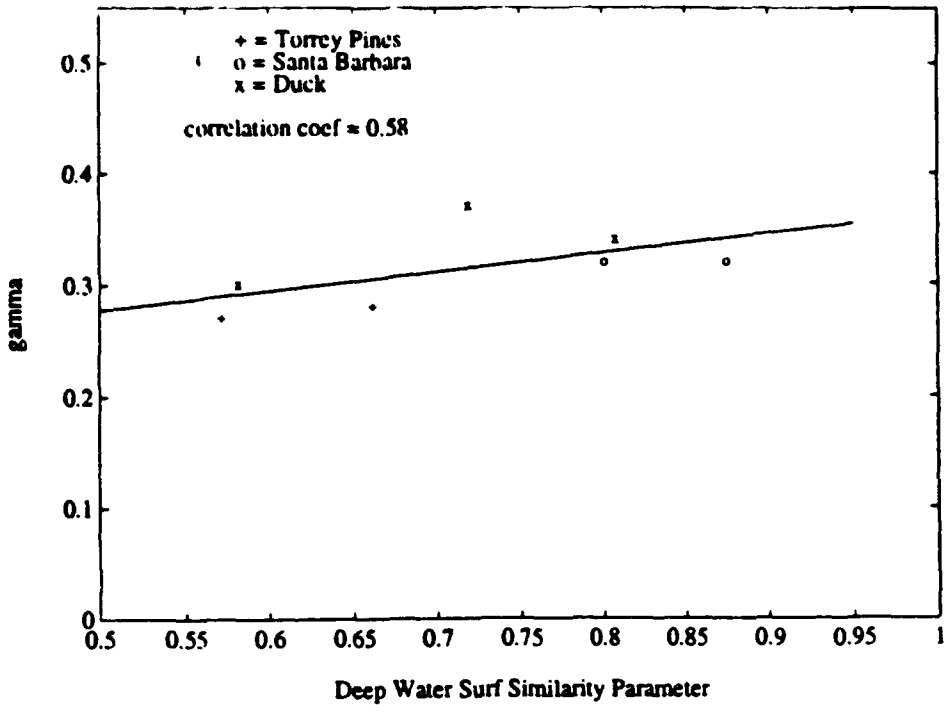

Figure 16. Correlation of γ and the deep water surf similarity parameter.

INITIAL DISTRIBUTION LIST

	No.Copies
1. Defense Technical Information Center Cameron Station Alexandria, VA 22304-6145	2
2. Library, Code 52 Naval Postgraduate School Monterey, CA 93943-5002	2
3. Chairman (Code 68Co) Department of Oceanography Naval Postgraduate School Monterey, CA 93943-5000	1
4. Chairman (Code 63Rd) Department of Meteorology Naval Postgraduate School Monterey, CA 93943-5000	1
5. Dr. E. B. Thornton (Code 68Tm) Department of Oceanography Naval Postgraduate School Monterey, CA 93943-5000	3
6 Dr. T. Lippmann (Code 68Tm) Department of Oceanography Naval Postgraduate School Monterey, CA 93943-5000	1
7 LT. A. Henry Brookins Naval Eastern Oceanographic Center Naval Air Station Norfolk, VA 23511	1
8. Director, Naval Oceanography Division Naval Observatory 34th and Massachusetts Avenue NW Washington, DC 20390	1
9. Commander Naval Oceanography Command Stennis Space Center MS 39529-5000	1

10. Commanding Officer 1
Naval Oceanographic Office
Stennis Space Center
MS 39529-5001

11. Office of Naval Research (Code 420) 1
Naval Ocean Research and Development Activity
800 N. Quincy Street
Arlington, VA 22217